

Fine Features of Optical Potential Well Induced by Nonlinearity

LEI-MING ZHOU^{1,*}, YAQIANG QIN^{2,3}, YUANJIE YANG⁴, AND YUQIANG JIANG^{2,3}

¹Department of Electrical and Computer Engineering, National University of Singapore, Singapore 117583, Singapore

²State Key Laboratory of Molecular Developmental Biology, Institute of Genetics and Developmental Biology, Chinese Academy of Sciences, Beijing, 100101, China

³University of Chinese Academy of Sciences, Beijing, 100049, China

⁴School of Physics, University of Electronic Science and Technology of China, Chengdu 610054, China

*Corresponding author: leiming.zhou@nus.edu.sg

Compiled November 12, 2020

Particles trapped by optical tweezers, behaving as mechanical oscillators in optomechanical system, have found tremendous applications in various disciplines and are still arousing research interests in frontier and fundamental physics. These optically trapped oscillators provide compact particle confinement and strong oscillator stiffness. But these features are limited by the size of the focused light spot of laser beams, which is typically restricted by the optical diffraction limit. Here, we propose to build optical potential well with fine features assisted by the nonlinearity of the particle material, which is independent of the optical diffraction limit. We show that the potential well shape can have super-oscillation-like features and Fano-resonance-like phenomenon, and the width of optical trap is far below the diffraction limit. The particle with nonlinearity trapped by ordinary optical beam provides a new platform with sub-diffraction potential well and can have applications in high accuracy optical manipulation and high precision metrology. © 2023 Optical Society of America

OCIS codes: (350.4855) Optical tweezers or optical manipulation; (190.3970) Microparticle nonlinear optics; (320.2250) Femtosecond phenomena.

<http://dx.doi.org/10.1364/XX.XX.XXXXXX>

Optical tweezers have found tremendous of applications in various areas, including colloidal sciences, chemistry and biophysics since its invention in several decades ago [1–4]. Especially, trapping with focused laser beams has advantages of non-contact, non-clamping and tunability. They are still arousing research interests in frontier and fundamental physics [5–12], such as obtaining negative pulling force [13, 14], searching non-Newtonian force [9], detecting gravitational wave [10], building quantum Carnot engine [11] and investigating the thermodynamics of non-equilibrium steady system [12]. In these researches, manipulating the particles in micro/nano-scale plays a key role. Trapping and manipulating particles in micro/nano-scale provide compact confinement, thus strong stiffness and

high frequency of the optical trapped oscillator. These features make high sensitivity metrology and the observation of micro-scale dynamics possible [5, 15].

However, the size of the focused light spot of laser beams is typically restricted by the optical diffraction limit [16]. Light spot (or the trapping potential well) with sub-diffraction size means that we can trap two particles away from each other while keeping the distance between them below the diffraction limit. This provides a way for parallel manipulation with compact size (particle arrangement below sub-diffraction at the same time) and high precision manipulation. Also, the width of the potential well will affect the stiffness of the trapped oscillator in optomechanical systems. Higher stiffness will increase the oscillation frequency and the sensitivity of the metrology applications based on the trapped oscillator. In order to obtain the sub-diffraction potential well, super-oscillation beams has been proposed to get smaller light spot [17–19]. Though super-oscillation beam can have a spot much smaller than the wavelength, the spot takes only a very minor part of the total incident power, which reduces the efficiency.

In those research above, the trapped particle or the oscillator is made of optical linear materials. Here, we investigate the trapping behaviors of particles with various high-order nonlinearities and report the building of a narrow potential well with width far below the diffraction limit. The proposal is based on the trapping theory of nonlinear particles. And recently, the effect induced by particle nonlinearity has been noticed with the introduction of the femtosecond light pulse [20–22]. Though the nonlinear coefficient of the particle is small, the strong light intensity of femtosecond laser beam makes the nonlinearity induced effect observable. The theory here then can be verified with the developing experiment techniques in the near future.

This paper is organized as follows. First, we describe the system investigated and the method used. Second, we show that different orders of nonlinearity exert different effects on the system. The potential well function can have Fano-resonance-like phenomenon and super-oscillation-like fine features. Then, we discuss the the experiment realization and validity of our theory.

Typically, gradient force generated by a light spot is used in

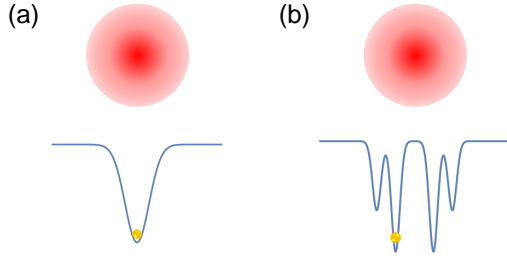


Fig. 1. Illustration of the optical potential well for (a) linear particle and (b) nonlinear particle in a single light spot.

optical trapping of micro/nano particles. Without loss of generality, we use a linear polarized Gaussian laser beam to represent this light spot, where the electromagnetic field has transverse distribution of the form $E(\rho) = |\mathbf{E}| = E_0 e^{-\rho^2}$. The radial distance from the center is denoted by ρ and the amplitude of the electric field in the center is E_0 . The wave-vector of the incident beam is k_m in the particle's surrounding medium, where $k_m = n_m k_0 = 2\pi n_m / \lambda_0$ and the wavelength in vacuum is λ_0 . The refractive index of the particle and the surrounding medium are n_p and n_m respectively. For a small spherical particle with radius a fulfilling the Rayleigh approximation (i.e., $k_m a \ll 1$ and $n_p k_0 a \ll 1$), the gradient force exerted by the electromagnetic field is $F = \frac{1}{4} \varepsilon_m \varepsilon_0 \text{Re}(\alpha) \nabla |\mathbf{E}|^2$. Here, $\alpha = \alpha_0 / (1 - ik_m^3 \alpha_0 / 6\pi \varepsilon_m)$ is the effective polarizability of the particle, $\alpha_0 = 4\pi a^3 \frac{\varepsilon_r - 1}{\varepsilon_r + 2}$ is the static polarizability [16, 23] and $\varepsilon_r = \varepsilon_p / \varepsilon_m$ is the relative refractive index. The phenomenological potential function is defined as $U(\rho) = -\int F(\rho) d\rho$. It's noted here that we consider the gradient force only to make the analysis of the trapping mechanism clearer. In the experiment, the scattering force should be eliminated by a counter-propagating beam. Otherwise, the analysis here is valid only on the radial direction on the transverse plane of the beam waist. For a particle with linear optical material, the polarizability is independent of the location, thus we have $U = -\frac{1}{4} \varepsilon_m \varepsilon_0 \text{Re}(\alpha) |\mathbf{E}|^2$. The shape of the trapping potential thus is the same with the profile of the light spot, which has a size limited by the diffraction limit (illustrated qualitatively by Fig. 1(a)).

However, for a particle with nonlinear optical material, the effective polarizability α depends on E (thus also dependent on particle location ρ). The susceptibility of the particle material with high order nonlinearity in a light spot is location dependent and reads

$$\chi(\rho) = \chi^{(1)} + \chi^{(3)} E^2 + \chi^{(5)} E^4 + \dots \quad (1)$$

Considering a field distribution with Gaussian shape in its transverse plane as before, the permittivity ($\varepsilon = 1 + \chi$) of the particle is also location dependent and reads

$$\varepsilon(\rho) = \varepsilon_1 + \Delta\varepsilon_3 e^{-2\rho^2} + \Delta\varepsilon_5 e^{-4\rho^2} + \dots \quad (2)$$

Among Eq. (2), $\varepsilon_1 = 1 + \chi^{(1)}$ and different orders of nonlinear coefficient cause different permittivity changes and are denoted as $\Delta\varepsilon_i = \chi^{(i)} E_0^{i-1}$ ($i = 3, 5, 7, \dots$) respectively. And finally, the effective polarizability α of the particle is location dependent, which induces changes in the potential function as illustrated qualitatively in Fig. 1(b).

Though the accurate potential function can be calculated with numerical integration of force F , we provide an approximate

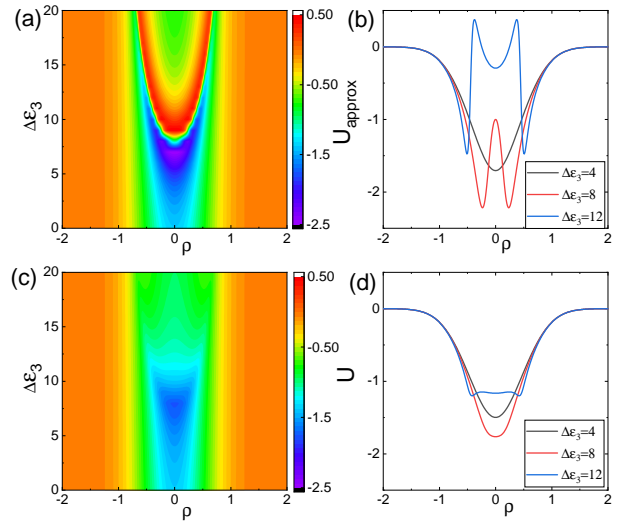


Fig. 2. The normalized potential for various nonlinearity when only the third order nonlinearity $\chi^{(3)}$ is included. (a) Approximate explicit potential U_{approx} for different $\Delta\varepsilon_3$ when $\varepsilon_1' = -10$ and $\varepsilon_1'' = 1.0$. (b) Potential well shape for U_{approx} with several different $\Delta\varepsilon_3$. (c-d) The same as Figs. (a-b) for accurate potential U calculated with numerical integration.

analytical expression to investigate it first. Suppose the location dependence of the permittivity $\varepsilon(\rho)$ is much less than that of the electrical field and the polarizability $\alpha \approx \alpha_0$ for a Rayleigh particle, the approximate potential function thus is

$$U_{\text{approx}} = -c_1 \text{Re} \left(\frac{\varepsilon_r(\rho) - 1}{\varepsilon_r(\rho) + 2} \right) |\mathbf{E}|^2. \quad (3)$$

Among Eq. (3), $c_1 = \pi a^3 \varepsilon_m \varepsilon_0$ is independent of the particle location and we takes it as a normalization coefficient of the potential function. This approximate expression is different from the accurate numerical result sometimes as shown later, because we have supposed the location dependence of the permittivity $\varepsilon(\rho)$ is much less than that of the electrical field. But it provides us a guidance to predict the main behaviors of the potential-well. Now, we show the results for various order of nonlinearity and their effects. Without loss of generality, it is supposed that the permittivity of the surrounding medium ε_m equals 1 (thus $\varepsilon_r = \varepsilon_p$) below.

For particles with only the third order nonlinearity coefficient $\chi^{(3)}$, the permittivity change is $\Delta\varepsilon = \Delta\varepsilon_3 e^{-2\rho^2} = \chi^{(3)} E_0^2 e^{-2\rho^2}$. The particle's linear relative permittivity is $\varepsilon_1 = \varepsilon_1' + i\varepsilon_1''$, where the real and imaginary part of the permittivity are denoted with ε_1' and ε_1'' respectively. The normalized potential function thus reads

$$\begin{aligned} U_{\text{approx}} &= -\text{Re} \left(\frac{\varepsilon_1' + i\varepsilon_1'' + \Delta\varepsilon_3 e^{-2\rho^2} - 1}{\varepsilon_1' + i\varepsilon_1'' + \Delta\varepsilon_3 e^{-2\rho^2} + 2} \right) e^{-2\rho^2} \\ &= -e^{-2\rho^2} + \frac{3e^{-2\rho^2} (\varepsilon_1' + \Delta\varepsilon_3 e^{-2\rho^2} + 2)}{(\varepsilon_1' + \Delta\varepsilon_3 e^{-2\rho^2} + 2)^2 + \varepsilon_1''^2} \\ &\triangleq U_{\text{linear}} + U_{\text{nonlinear}}^{(3)}. \end{aligned} \quad (4)$$

It can be seen that the linear potential function U_{linear} keeps the Gaussian shape, while the nonlinear potential $U_{\text{nonlinear}}^{(3)} =$

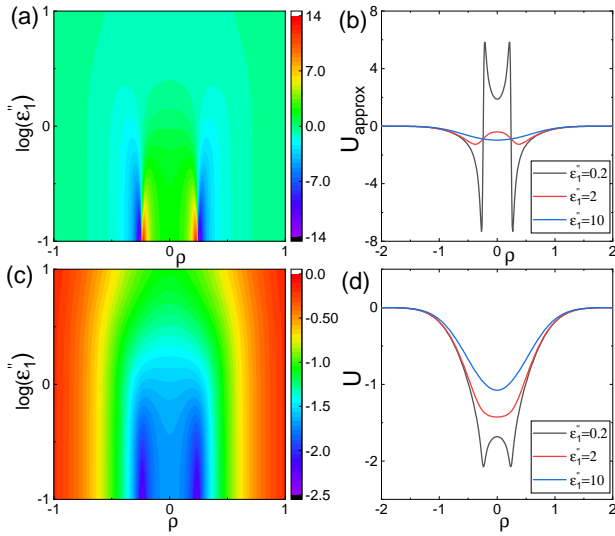


Fig. 3. The normalized potential for various absorption when only the third order nonlinearity $\chi^{(3)}$ is included. (a) Approximate explicit potential U_{approx} for different ϵ_1'' when $\epsilon_1' = -10$ and $\Delta\epsilon_3 = 9$. (b) Potential well shape for U_{approx} with several different $\Delta\epsilon_3$. (c-d) The same as (a-b) for accurate potential U calculated with numerical integration.

$3e^{-2\rho^2}U_{\text{core}}^{(3)}$ shows a Fano-like shape core with a Gaussian envelop, as shown in Fig. 2(a-b). When $\Delta\epsilon_3$ (proportional to $\chi^{(3)}$) increases, the potential function changes from single potential well to double potential well, and even get a third potential well in the center (when $\Delta\epsilon_3 = 12$ as shown in Fig. 2(a)). Accurate potential well U got from the numerical integration of force F arrives the similar result as shown in Fig. 2(c-d). The potential well changes from single well to double well as predicted, and the location of the double well coincides with the approximation result for cases where the $\Delta\epsilon_3$ is away from the just splitting point.

The core function $U_{\text{core}}^{(3)} = \frac{\epsilon_1' + \Delta\epsilon_3 e^{-2\rho^2} + 2}{(\epsilon_1' + \Delta\epsilon_3 e^{-2\rho^2} + 2)^2 + \epsilon_1''^2}$ shows its maximum/minimum values $\pm \frac{1}{2\epsilon_1''}$ when $\epsilon_1' + \Delta\epsilon_3 e^{-2\rho^2} + 2 = \pm \epsilon_1''$. These points are also the points of the maximum/minimum of the Fano-like shape of potential function. The depth and width of the potential well is different from the approximate analytical result, which is mainly affected by the imaginary part of the permittivity ϵ_1'' as we will show below. We also show the corresponding normalized force F for various $\Delta\epsilon_3$ in Fig. 4(a) as a reference. In the numerical calculation, $a = 30$ nm and $\lambda_0 = 840$ nm. However, as long as the Rayleigh approximation is fulfilled, the radius of the particle doesn't affect the shape of the normalized potential well in fact.

While $\Delta\epsilon_3$ determines the location of the transition point, the absorption part ϵ_1'' mainly affects the width and depth of the potential well. We show these behaviors of the shape of the potential well in Fig. 3(a-b) for various ϵ_1'' . It can be seen that when the absorption ϵ_1'' is small, the potential well depth increases very much and the Fano-like shape is pronounced. Large ϵ_1'' (i.e., large particle absorption) will flat the potential curve and even change the double well into single well. Numerical result shows similar behaviors and the flattening effect of the imaginary part

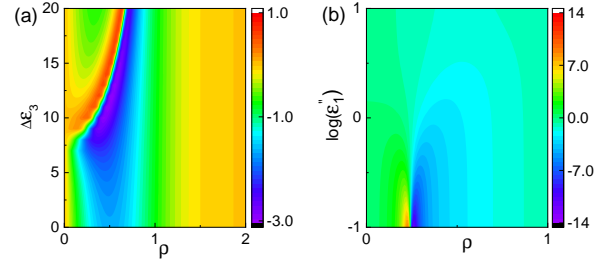


Fig. 4. (a) The normalized force $F(\rho)$ for different $\Delta\epsilon_3$ when $\epsilon_1' = -10$ and $\epsilon_1'' = 1.0$. (b) The normalized force $F(\rho)$ for different ϵ_1'' when $\epsilon_1' = -10$ and $\Delta\epsilon_3 = 9$.

of the permittivity is more obvious. The normalized force F for various ϵ_1'' is also shown in Fig. 4(b).

When the permittivity is real, the simplified potential reads

$$U_0 = -\left(1 - \frac{3}{\epsilon_1 + 2 + \Delta\epsilon_3 e^{-2\rho^2}}\right)e^{-2\rho^2}. \quad (5)$$

Among Eq. (5), there is a singular point when $\epsilon_1 + 2 + \Delta\epsilon_3 e^{-2\rho^2} = 0$. It is corresponding to the maximum/minimum point of the double-well potential function as mentioned above when ϵ_1'' is very small. This point has been experimentally observed before [20], where they used the gold nano-particle. For metallic particle such as gold particle, $\epsilon_1 + 2 < 0$ and $\Delta\epsilon_3 e^{-2\rho^2} > 0$.

If higher order nonlinearity is included, they change the part $\Delta\epsilon$ and the potential shape could have more details. Taking $\chi^{(5)}$ as an example, the normalized potential function reads

$$\begin{aligned} U_{\text{approx}} &= -\text{Re}\left(\frac{\epsilon_1' + i\epsilon_1'' + \Delta\epsilon_3 e^{-2\rho^2} + \Delta\epsilon_5 e^{-4\rho^2} - 1}{\epsilon_1' + i\epsilon_1'' + \Delta\epsilon_3 e^{-2\rho^2} + \Delta\epsilon_5 e^{-4\rho^2} + 2}\right)e^{-2\rho^2} \\ &= -e^{-2\rho^2} + \frac{3e^{-2\rho^2}(\epsilon_1' + \Delta\epsilon_3 e^{-2\rho^2} + \Delta\epsilon_5 e^{-4\rho^2} + 2)}{(\epsilon_1' + \Delta\epsilon_3 e^{-2\rho^2} + \Delta\epsilon_5 e^{-4\rho^2} + 2)^2 + \epsilon_1''^2} \\ &\triangleq U_{\text{linear}} + U_{\text{nonlinear}}^{(5)}. \end{aligned} \quad (6)$$

The nonlinear potential $U_{\text{nonlinear}}^{(5)} = 3e^{-2\rho^2}U_{\text{core}}^{(5)}$ also has a Gaussian envelop. If the sign of $\chi^{(5)}$ is the same as that of $\chi^{(3)}$, it doesn't change the shape of the total nonlinearity-induced permittivity $\Delta\epsilon$ because $\Delta\epsilon_3 e^{-2\rho^2}$ and $\Delta\epsilon_5 e^{-4\rho^2}$ have the same monotonicity. Thus the potential shape keeps the same as the case of $\chi^{(3)}$. However, $\chi^{(5)}$ with opposite sign will show more oscillations as shown in Fig. 5(a-b). As shown in Fig. 5(b), the potential function shows a super-oscillation-like behavior with chosen parameters. For a strongly focused light spot, the total width of the Gaussian envelop is limited by the diffraction limit and thus the single wells in this super-oscillation-like potential well will have width far below the diffraction limit.

More higher order nonlinearities cannot introduce more oscillations. All the changed permittivity terms ($\Delta\epsilon_i e^{-(i-1)\rho^2}$) can be gathered together into two groups, according to the sign of the nonlinearity coefficient. All the terms associated with positive/negative high-order nonlinearities shows the same monotonicity when the location of the particle changes. Then the behaviors induced by all the nonlinearities are the same as the case where only $\chi^{(3)}$ and $\chi^{(5)}$ are included.

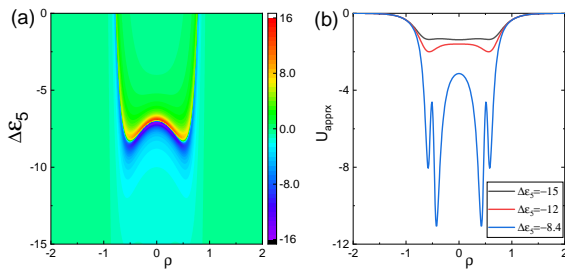


Fig. 5. (a) The normalized potential function U_{approx} for various $\Delta\epsilon_5$ when $\epsilon_1 = -5 + 0.1i$ and $\Delta\epsilon_3 = 10$. (b) Several representative potential-well function for different $\Delta\epsilon_5$. Higher-order nonlinearity can induce obvious super-oscillation-like potential function such as $\Delta\epsilon_5 = -8.4$.

The inclusion of even-order nonlinearities shows the same behaviors as we have found before. In the above discussion, we only consider odd-order nonlinearities for simplification because the material of the trapped particle is usually with central inversion symmetry. Materials with this symmetry have only zero even-order nonlinearities. However, even if we introduce even-order nonlinearities, they can be analyzed as what we did for higher order nonlinearities. Through grouping positive and negative nonlinearity coefficients, the total potential function show the same behaviors as when only $\chi^{(3)}$ and $\chi^{(5)}$ are included.

In discussion, we would like to investigate the experiment realization and validity of our theory. The nonlinearity of the material is usually small and it is hard to observe the nonlinearity induced trapping effect. But the ultra-high light intensity can induce enough permittivity change [20, 21, 24–28] and the potential well splitting using gold particle has been demonstrated with the aid of femtosecond pulse laser [20, 21]. Thus we discussed metallic particles as examples in the study above, where the particle permittivity is negative. It's noted that the high light intensity may damage the particle because of heating. However, we believe two factors will still promise the experimental verification. The first one is the material with no central-inversion symmetry. In this case, materials can have even order nonlinearity, such as $\chi^{(2)}$. As effects of $\chi^{(3)}$ has already been observed, material with $\chi^{(2)}$ and $\chi^{(3)}$ can show the phenomena we discussed here within the reach. The second one is the developing material science and realization of meta-materials [29]. Artificial materials with desired high-order nonlinearity will demonstrate the theory here under lower light intensity in the future. Finally, we would like to mention that we discussed the materials with scalar nonlinearity coefficients in this work, which is true for homogeneous and isotropic materials. For anisotropic materials, the nonlinearity coefficient is a tensor. The trapping will then have more colorful phenomena deserved future investigations.

In summary, we investigated the features of the potential well of an optically trapped particle with various orders of nonlinearity. The potential well shape can have super-oscillation-like features and Fano-resonance-like phenomenon, which provides finer particle confinement far beyond the optical diffraction limit. It provides a new method to manipulate micro/nano-particles parallel with sub-diffraction distance and may build a platform for high sensitivity measurement in opto-mechanical system.

Acknowledgment. We acknowledge the support from Ministry of Education, Singapore (Grant No. R-263-000-D11-114) and discussions with Cheng-Wei Qiu. Y. Y. acknowledges sup-

port of National Natural Science Foundation of China (11874102), Sichuan Province Science and Technology Support Program (20CXRC0086). Y. Jiang acknowledges support from the Strategic Priority Research Program of Chinese Academy of Sciences (Grant no. XDA24020202) and partial support from the National Natural Science Foundation of China (No. 11674389).

Disclosures. The authors declare no conflicts of interest.

REFERENCES

1. A. Ashkin, J. M. Dziedzic, J. E. Bjorkholm, and S. Chu, *Opt. Lett.* **11**, 288 (1986).
2. D. G. Grier, *Nature*. **424**, 810 (2003).
3. K. Dholakia and P. Zemánek, *Rev. Mod. Phys.* **82**, 1767 (2010).
4. C.-W. Qiu and L.-M. Zhou, *Light. Sci. Appl.* **7**, 86 (2018).
5. T. Li, S. Kheifets, D. Medellin, and M. G. Raizen, *Science*. **328**, 1673 (2010).
6. T. Li, S. Kheifets, and M. G. Raizen, *Nat. Phys.* **7**, 527 (2011).
7. Z.-Q. Yin, A. A. Geraci, and T. Li, *Int. J. Mod. Phys. B* **27**, 1330018 (2013).
8. L.-M. Zhou, K.-W. Xiao, J. Chen, and N. Zhao, *Laser Photonics Rev.* (2017).
9. A. A. Geraci, S. B. Papp, and J. Kitching, *Phys. Rev. Lett.* **105**, 101101 (2010).
10. A. Arvanitaki and A. A. Geraci, *Phys. Rev. Lett.* **110**, 071105 (2013).
11. I. A. Martínez, É. Roldán, L. Dinis, D. Petrov, J. M. R. Parrondo, and R. A. Rica, *Nat. Phys.* **12**, 67 (2016).
12. J. Gieseler, R. Quidant, C. Dellago, and L. Novotny, *Nat. Nanotechnol.* **9**, 358 (2014).
13. W. Ding, T. Zhu, L.-M. Zhou, and C.-W. Qiu, *Adv. Photonics* **1**, 1 (2019).
14. H. Li, Y. Cao, L.-M. Zhou, X. Xu, T. Zhu, Y. Shi, C.-W. Qiu, and W. Ding, *Adv. Opt. Photonics* **12**, 288 (2020).
15. L.-M. Zhou, K.-W. Xiao, Z.-Q. Yin, J. Chen, and N. Zhao, *Opt. Lett.* **43**, 4582 (2018).
16. P. Jones, O. Maragó, and G. Volpe, *Optical tweezers: Principles and applications* (Cambridge University Press, 2015).
17. B. K. Singh, H. Nagar, Y. Roichman, and A. Arie, *Light. Sci. Appl.* **6**, e17050 (2017).
18. G. Chen, Z.-Q. Wen, and C.-W. Qiu, *Light. Sci. Appl.* **8**, 56 (2019).
19. H. Nagar, T. Admon, D. Goldman, A. Eyal, and Y. Roichman, *Opt. Lett.* **44**, 2430 (2019).
20. Y. Jiang, T. Narushima, and H. Okamoto, *Nat. Phys.* **6**, 1005 (2010).
21. Y. Zhang, J. Shen, C. Min, Y. Jin, Y. Jiang, J. Liu, S. Zhu, Y. Sheng, A. V. Zayats, and X. Yuan, *Nano Lett.* **18**, 5538 (2018).
22. L. Huang, Y. Qin, Y. Jin, H. Shi, H. Guo, L. Xiao, and Y. Jiang, *Nanophotonics*. **9**, 4315 (2020).
23. K. Svoboda and S. M. Block, *Opt. Lett.* **19**, 930 (1994).
24. A. Usman, W.-Y. Chiang, and H. Masuhara, *Sci. Prog.* **96**, 1 (2013).
25. A. Devi and A. K. De, *Phys. Rev. A* **96**, 1 (2017).
26. L. Gong, B. Gu, G. Rui, Y. Cui, Z. Zhu, and Q. Zhan, *Photonics Res.* **6**, 138 (2018).
27. H. Q. Quy, D. Q. Tuan, T. D. Thanh, and N. M. Thang, *Opt. Commun.* **427**, 341 (2018).
28. A. Devi, S. S. Nair, and A. K. De, *EPL*. **126**, 28002 (2019).
29. G. Hu, X. Hong, K. Wang, J. Wu, H.-X. Xu, W. Zhao, W. Liu, S. Zhang, F. Garcia-Vidal, B. Wang, P. Lu, and C.-W. Qiu, *Nat. Photonics* **13**, 467 (2019).